Article type: A-Regular research paper

First principles calculations of electronic and optical properties for mixed perovskites: $Ba_{(1-x)}Ca_{(x)}TiO_3$ and $Ba_{(1-x)}Sr_{(x)}TiO_3$ (x=0.4, 0.6)

O. Tahiri, S. Kassou, R. El Mrabet & A. Belaaraj

Laboratoire Physique des Matériaux et Modélisation des Systèmes, CNRST-URAC08, Département de physique, Faculté des Sciences, Université Moulay Ismail, 50000-Meknes, Maroc.

Corresponding author: a.belaaraj@fs-umi.ac.ma

Abstract: The effect of Ca and Sr-doping on the structural electronic and optical properties of the cubic $Ba_{1-x}Ca_xTiO_3$ and $Ba_{1-x}Sr_xTiO_3$ (x=0.4, 0.6) mixed crystals was investigated using first-principles calculations based on density functional theory (DFT). The calculated band structures based on the optimized geometry of the cell for the solid solutions show an indirect band gap character at M-points, with low energy dispersion along height symmetry directions in the Brillouin zone. The band gaps increase with Ca and Sr concentrations. The total and partial densities of states were analyzed to examine the contribution of different orbitals to the maximum of valence band and the minimum of the conduction band. The optical properties such as reflectivity, energy loss, refractive index and extinction coefficient were studied.

Keywords: DFT CALCULATIONS, BAND GAP, DENSITY OF STATE, OPTICAL PROPERTIES.

Introduction

The interest carried in perovskites ($ATiO_3$) and their dielectric properties did not stop growing. The technico-economics requirements, directed essentially to the miniaturization and the production at a lower cost, are at the origin of the discovery of new successful materials. The most recent fields of application are the ones of the aeronautics, the antennas guides of waves, filters, satellite links, the processing and storage of the information [1-3].The titanate of barium is certainly the material most studied among compounds ferroelectrics [4] due to their chemical and mechanical stability. At room temperature it exhibit a ferroelectric properties in tetragonal phase with space group P4mm, over this temperature the $BaTiO_3$ becomes a cubic phase Pm-3m.

The integration of ions isovalents as, Ca^{2+}, Sr^{2+} and Pb^{2+} in Ba sites and the substitution of tetravalent ions Ti^{4+} by Zr^{4+}, Sn^{4+} and Hf^{4+} can influences the properties of the $BaTiO_3$, such as the phase transition temperature and tailor these properties to performance requirements. The investigations in this domain were mainly concentrated on the systems (Ba, Sr)TiO_3 characterized by high dielectric constant. Increasing content of Sr^{2+} on the Ba^{2+} site, leads to decrease the temperature transition with an expansion of the constant dielectric, low leakage current, low dielectric dispersion against frequency and can be implanted in electroluminescent devices as a high transparency insulator layer [5].

The major problems of these compounds seem of dielectric losses and its relative variation, according to the temperature [6,7]. In order to reduce this inconvenient, we have considered the good dielectric properties and the relaxor nature of (Ba, Ca) TiO_3 materials which are expected as alternative candidates fortunable microwave dielectric materials with low dielectric loss and temperature dependence.

The aim of this work is to carry out the electronic and optical properties;

such as reflectivity, energy loss, refractive index and extinction coefficient of $Ba_{1-x}Ca_xTiO_3$ and $Ba_{1-x}Sr_xTiO_3$, where x = 0.4 and 0.6, using the first principle calculations.

Computation detail

We used for our calculations ABINIT ab initio software package [8-10] which is based on the density functional theory (DFT), using plane wave pseudo potential formalism, in order to obtain response function calculations [11-13], computing are performed by the generalized gradient approximation (GGA) with the Fritz-Haber-Institute (FHI) pseudopotentials and Perdew-Burke-Ernzerh of exchange correlation [14], energy cutoff of the electronic wave functions was expanded in plane waves at 950 eV, which are well converged. The Monkhorst Pack Mesh scheme [15] k-points grid sampling was set at 4 x 4 x 4 to perform the irreducible Brillouin zone integrations. The initial crystal data of $BaTiO_3$ in cubic structure with the space group Pm-3m reported in the literature [16], were used as a starting point. The optimized structure and minimum energy lattice constants of the relaxed cubic unit cell were initially computed. The electronic and optical properties were calculated for the equilibrium structures.

Structural and electronic properties

The calculated a-cell parameters are listed in Table1. It is apparent that the a-lattice parameter decreases with doped amount of the Sr and Ca elements, this result is due to the lower ionic radius value of Sr and Ca compared to Ba in the pure compound $BaTiO_3$. The values obtained for the pure $BaTiO_3$, $SrTiO_3$ and $CaTiO_3$ crystals are in perfect agreement with other theoretical and experimental values [17-19].

Table 1: Calculated a-cell parameter and band gap energy of Ca and Sr-substitued BaTiO3

	Cell parameter(a) (Å)	Band gap Eg (eV)
BaTiO₃	4.123	2.150
	4.008 [17]	2.200 [23] Ahuja
	4.011 [16] Exp	3.270 [26] Exp
Ba₀.₆Ca₀.₄TiO₃	4.106	2.201
Ba₀.₄Ca₀.₆TiO₃	4.075	2.263
CaTiO₃	3.964	2.433
	3.851[17]	2.780 [24]
	3.895[18] Exp	3.500 [27] Exp
Ba₀.₆Sr₀.₄TiO₃	4.092	2.222
Ba₀.₄Sr₀.₆TiO₃	4.064	2.266
SrTiO₃	3.984	2.380
	3.907 [17]	2.200 [23]
	3.890 [18] Exp	3.250 [28] Exp

The calculated band structures along the high symmetry directions in the first irreducible Brillouin Zone, in the same scale from -6 eV to 20 eV for all crystals are shown in figure1; these bands look very similar and agree with band structure published, previously in the literature [17-23]. The nature of the crystal components and the electrostatic interactions affect the dispersion of the band structure. The top of the valence band, for $Ba_{0.6}Ca_{0.4}TiO_3$, $Ba_{0.4}Ca_{0.6}TiO_3$, $Ba_{0.6}Sr_{0.4}TiO3$ and $Ba_{0.4}Sr_{0.6}TiO_3$ compounds, is located at M-points. The highest valence states at M-points appear only about 0.1 eV after the highest states at points. The bottom of the conduction band is located at -points. The lowest valence states at - points appear only about 0.1 eV after the highest states at X-points. The analysis of all directions reveals medium energy dispersion along -M and M-X directions, while a lower dispersion is present along -X, equivalent to the revolution axis.
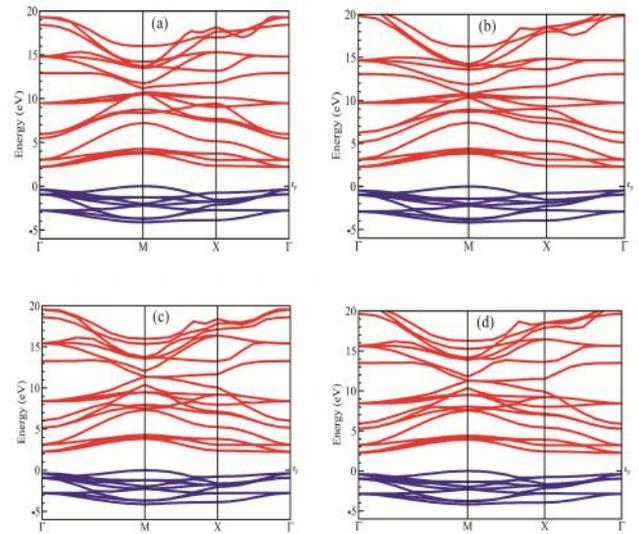

Figure 1: Calculated band structure: a) Ba₀.₆Ca₀.₄TiO₃, b) Ba₀.₆Sr₀.₄TiO₃, c) Ba₀.₄Ca₀.₆TiO₃, d) Ba₀.₄Sr₀.₆TiO₃

The figures reveal also that all compounds exhibit an indirect band gap transition. From Table 1, we can see that the energy gap increases by increasing the Ca and Sr content. This effect of doping is in agreed with previous works [19,20]. The high band gap value is found to be 2.266 eV for $Ba_{0.4}Sr_{0.6}TiO_3$. The calculated values for the pure $BaTiO_3$, $SrTiO_3$ and $CaTiO_3$ (Figure 2) are found to be 2.15 eV, 2.380 eV and 2.433 eV respectively, which are in reasonable agreement with other theoretical data [21-24]. While they are slightly lower than available experimental results [26-28]. These results are well known by underestimate the band gap presented by DFT calculations [29-31].

Figure 3 shows plots of the total (TDOS) and partial (PDOS) densities of states for $Ba_{0.4}Ca_{0.6}TiO_3$, $Ba_{0.4}Sr_{0.6}TiO_3$, $Ba_{0.6}Ca_{0.4}TiO_3$ and $Ba_{0.6}Ca_{0.4}TiO_3$. A low displacement of the density is observed in conduction band to high energy as function of Ca and Sr concentration.

The analysis of TDOS and PDOS variation versus photon energy reveals that the maximum of the valence band is occupied by the orbital O-2p, and the minimum of the conduction band is occupied by the orbital Ti-3d. From -4 eV to -1 eV, appears the mixed contribution of O-2p, Ti-3d and a low contribution of Ba-6s, Ca-4s and Sr-5s orbitals. Beyond 6 eV, a low contribution of O-2s, O-2p, Ti-3s, Ti-3d, Ba-5p, Ba-6s, Ca-3p, Ca-4s, Sr-5s and Sr-4p orbitals appears too.

Optical properties

The real and imaginary components of the dielectric function are used to calculate the optical properties of $Ba_{1-x}Ca_xTiO_3$ and $Ba_{1-x}Sr_xTiO_3$ solid solutions, such as the reflectivity R ( ), energy loss L( ), refractive index n ( )and extinction coefficient k ( ) from the following relationships [22]:

$$R(\ ) = \left| \frac{\sqrt{(\ )} - 1}{\sqrt{(\ )} + 1} \right|^2$$

$$L(\ ) = \frac{_2(\ )}{_1(\ )^2 + _2(\ )^2}$$

$$k(\ ) = \frac{1}{\sqrt{2}} \left[\sqrt{_1(\ )^2 + _2(\ )^2} - _1(\ ) \right]^{1/2}$$

$$n(\ ) = \frac{1}{\sqrt{2}} \left[\sqrt{_1(\ )^2 + _2(\ )^2} + _1(\ ) \right]^{1/2}$$

Where $_1(\ )$ and $_2(\ )$ are the real and imaginary parts of the frequency
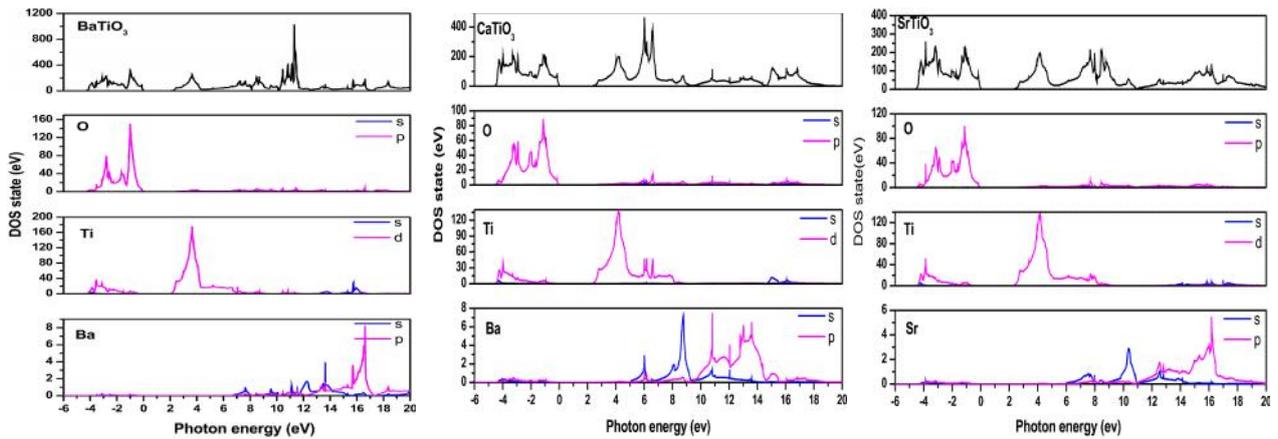
Figure 2: Total and partial densities of states of the pure $BaTiO_3$, $CaTiO_3$ and $SrTiO_3$
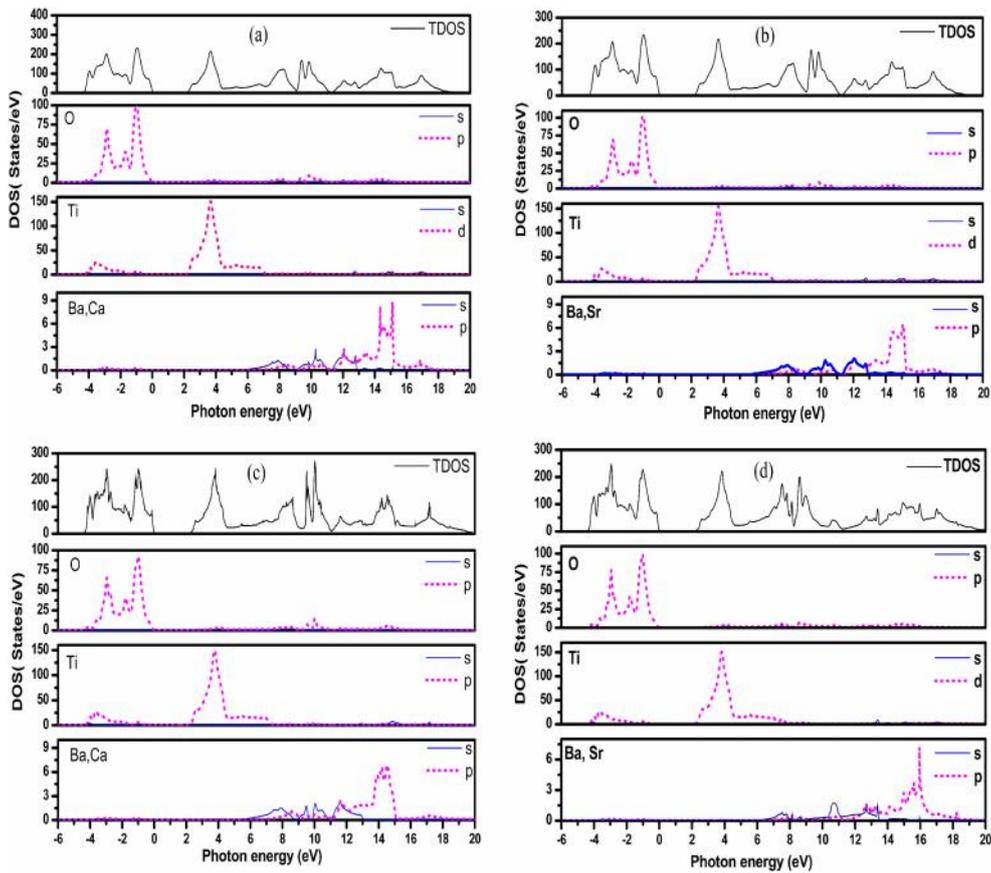

Figure 3: Total and partial densities of states: a) $Ba_{0.6}Ca_{0.4}TiO_3$, b) $Ba_{0.6}Sr_{0.4}TiO_3$, c) $Ba_{0.4}Ca_{0.6}TiO_3$, d) $Ba_{0.4}Sr_{0.6}TiO_3$

complex dielectric function $(\omega) = \epsilon_1(\omega) + i\epsilon_2(\omega)$, which are calculated from the Kramers-Kronig relationship and the momentum matrix elements between the occupied and unoccupied wave functions[32-33].

The calculated reflectivity $R(\omega)$ of the studied compounds, in the energy range from 0 to 30 eV, are shown in figure 4 For the energy values less than 1 eV and above 22 eV, the reflectivity is lower than 17% for all compounds, which indicates that these compounds are transparent, and expected to be poor electrical conductors at this range.
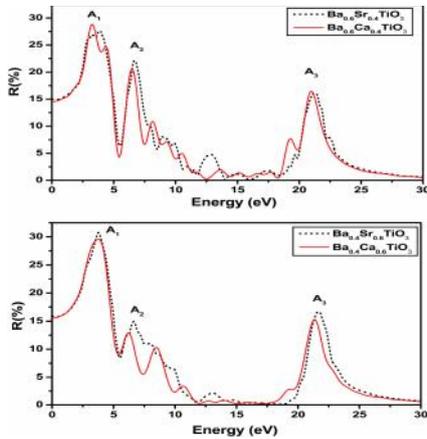
Figure 4: Variation of reflectivity R(ω) versus photon energy: a) Ba₀.₆Ca₀.₄TiO₃ and Ba₀.₆Sr₀.₄TiO₃- b) Ba₀.₄Ca₀.₆TiO₃ and Ba₀.₄Sr₀.₆TiO₃

The curves show that the first optical critical point (A_1) of the reflectivity occurs at 3.271 eV and 3.790 eV for $Ba_{0.6}Ca_{0.4}TiO_3$ and $Ba_{0.4}Ca_{0.6}TiO_3$, and at 3.907 eV and 3.790 eV for $Ba_{0.6}Sr_{0.4}TiO_3$ and $Ba_{0.4}Sr_{0.6}TiO_3$. These points give the threshold for indirect optical transitions between the valence band (VB) and the conduction band (CB), which are known as the fundamental absorption edge due to the interaction between the O-2p and Ti-3d states [34-35]. After this threshold energy (first critical point), the curves decrease towards another critical point A_2, this peak is caused by the interaction between the O-2p and higher-energy conduction bands, whereas the peak A_3 is due to the interactions between Ti-3d and O-2s. We can observe that the first peaks resulting from transition between O-2p and Ti-3d are dominant.
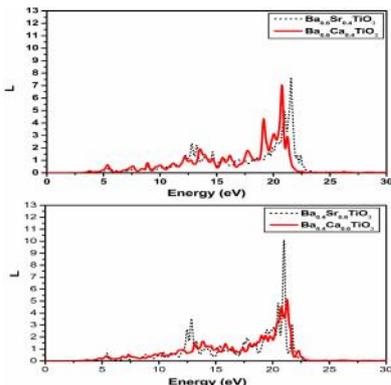

Figure 5: Variation of energy loss L(ω) versus photon energy: a) Ba₀.₆Ca₀.₄TiO₃ and Ba₀.₆Sr₀.₄TiO₃- b) Ba₀.₄Ca₀.₆TiO₃ and Ba₀.₄Sr₀.₆TiO₃

As shown in figure 5, the energy loss gives a sharp peak at 21 eV, which is related with the reduction of reflectivity $R(\omega)$, and gives the plasma frequency ω_p, according to Drude theory [36].
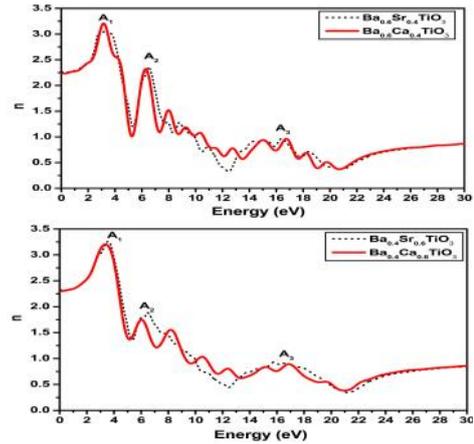

Figure 6: Variation of refractive index n(ω) versus photon energy: a) Ba₀.₄Ca₀.₆TiO₃ and Ba₀.₄Sr₀.₆TiO₃ b) Ba₀.₆Ca₀.₄TiO₃ and Ba₀.₆Sr₀.₄TiO₃

The variation of refractive index $n(\omega)$, with photon energy, for the titled compounds are shown in figure 6. At 0 frequency, the value of the refractive index is found to be about 2.25 for $Ba_{0.6}Ca_{0.4}TiO_3$ and $Ba_{0.6}Sr_{0.4}TiO_3$, and 2.30 for $Ba_{0.4}Ca_{0.6}TiO_3$ and $Ba_{0.4}Sr_{0.6}TiO_3$. Their variations enhanced beyond the zero frequency, increase with energy in transparency region and limit reaching their maximum values in the UV region at A_1 point. The obtained values are 3.204 for $Ba_{0.6}Ca_{0.4}TiO_3$, 3.201 for $Ba_{0.4}Ca_{0.6}TiO_3$, 3.040 for $Ba_{0.6}Sr_{0.4}TiO_3$ and 3.258 for $Ba_{0.4}Sr_{0.6}TiO_3$. Beyond the maximum point (A_1), the refractive index decreases with few oscillations to A2 and A3 points. Then, it tend to the unity after plasma frequency which exhibit an insulators-like behaviour. In general, the spectra are shifted towards low energies by changing the cations from Ba to Ca and Sr.

The calculated extinction coefficient $k(\omega)$ for $Ba_{0.6}Ca_{0.4}TiO_3$ and $Ba_{0.4}Sr_{0.6}TiO_3$ and for $Ba_{0.6}Ca_{0.4}TiO_3$ and $Ba_{0.4}Sr_{0.6}TiO_3$ is displayed in figure 7a and figure 7b respectively. The analysis of the curves depicts a constant value between 0 eV and the optical edge value, and then, the extinction coefficient increases with Ca and Sr content, accompanied by some swings which are due to the extinction of the plasmons. The absorption edge starts from about 2 eV, corresponding to the energy gap. This originates from the transition between O-2p states located at the top of the valence bands to the Ti-3d states dominating in the bottom of the conduction bands. Table II gathers the values of the critical points (A1). The higher value was observed for $Ba_{0.4}Ca_{0.6}TiO_3$ (1.970 at 4.485 eV).
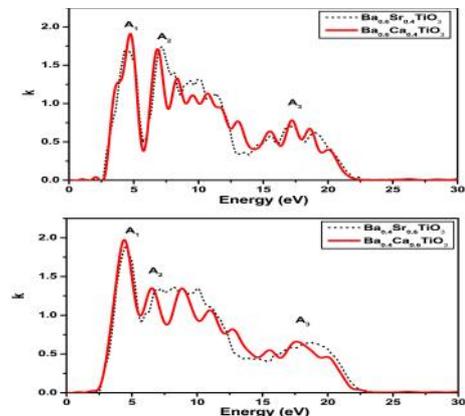

Figure 7: Variation of extinction coefficient k(ω) versus photon energy: a) Ba₀.₆Ca₀.₄TiO₃ and Ba₀.₆Sr₀.₄TiO₃ b) Ba₀.₄Ca₀.₆TiO₃ and Ba₀.₄Sr₀.₆TiO₃

Table 2. Maximum values of the first peaks for optical constants.

	R (Š)		n (Š)		k (Š)	
	0.4	**0.6**	**0.4**	**0.6**	**0.4**	**0.6**
$Ba_{1-x}Ca_xTiO_3$	28.9	29.4	3.195	3.180	1.900	1.970
$Ba_{1-x}Sr_xTiO_3$	27.4	30.6	3.030	3.250	1.700	1.870

Conclusion

We have investigated the structural, electronic and optical properties of $Ba_{1-x}Ca_xTiO_3$ and $Ba_{1-x}Sr_xTiO_3$ (x=0.4, 0.6) using DFT calculations with GGA approximation as implemented in the ABINIT package. The results show that the fundamental gap of all compounds exhibits an indirect transition at M-points, with low energy dispersion along height symmetry directions wich is large compared to $BaTiO_3$ situated at Γ- point. The calculated energy band gaps are 2.201 eV, 2.222 eV, 2.263 eV and 2.266 eV for $Ba_{0.6}Ca_{0.4}TiO_3$, $Ba_{0.6}Sr_{0.4}TiO_3$, $Ba_{0.4}Ca_{0.6}TiO_3$ and $Ba_{0.4}Sr_{0.6}TiO_3$ respectively. The analysis of the total and partial densities of states reveals the contribution of all components around the energy gap and a small displacement of the density in conduction band to high energy. the energy loss gives a sharp peak at 21 eV, which is related with the reduction of reflectivity due to plasma frequency ω_p.

REFERENCES

1. R. Migoni, H. Bilz, D. Bauderle, *Origin of Raman scattering and ferroelectricity in oxidic perovskite, Physical Review Letters,* **vol. 37**, no 17, p. 1155. (1976).

2. G. Binning, H. E. Hoenig, *Energy gap of the superconducting semiconductor SrTiO3– x determined by tunneling, Solid State Communications*. **vol. 14**, no 7, p. 597-601. (1974).

3. K. Taibi, Some lead-free ceramics of ferroelectric and photoelectrochemical applications*, Materials and Devices,* **vol. 1,** no 1. (2017).

4. M. E. Lines, E. Malcolm, A. M .Glass, M. Alastair, *Principles and applications of ferroelectrics and related materials*, *Oxford university press.* (1977).

5. T. S. Kim, M. H. Oh, C. H. Kim, *Influences of Indium Tin Oxide Layer on the Properties of RF Magnetron-Sputtered (BaSr) TiO3 Thin Films on Indium Tin Oxide-Coated Glass Substrate, Japanese journal of applied physics*, **vol. 32,** no 6R, p. 2837. (1993).

6. B. L. Cheng, B. Su, J. E. Holmes, T. W. Button, M. Gabbay, G. Fantozzi, *Dielectric and mechanical losses in (Ba, Sr) TiO 3 systems*, *Journal of electroceramics,* **vol. 9**, no 1, p. 17-23, (2002).

7. H. Chang, I. Takeuchi, X. D. Xiang, *A low-loss composition region identified from a thin-film composition spread of (Ba 1– x– y Sr x Ca y) TiO₃, Applied Physics Letters*, **vol. 74**, no 8, p. 1165-1167. (1999).

8. X. Gonze, B. Amadon, P. M. Anglade, J. M. Beuken, F. Bottin, P. Boulanger, T. Deutsch, ABINIT *Computer Physics Communications*, **vol. 180**, no 12, p. 2582-2615. (2009).

9. X. Gonze, J. M. Beuken, R. Caracas, F. Detraux, M. Fuchs, G. M. Rignanese, M. Torrent, *First-principles computation of material properties: the ABINIT software project, Computational Materials Science*, **vol. 25**, no 3, p. 478-492, (2002).

10. www.abinit.org

11. P. Hohenberg and W. Kohn, *Inhomogeneous Electron Gas, Phys Rev.* **vol. 136**, no 3B, p. B864, (1964).

12. W. Kohn, L. J. Sham, *Self-consistent equations including exchange and correlation effects*, *Phys. Rev.* **vol. 140**, no 4A, p. A1133 (1965).

13. M.C. Payne, M.P. Teter, D.C. Allan, T. A. Arias, and J.D, *Iterative minimization techniques for ab initio total-energy calculations: molecular dynamics and conjugate gradients*, *Joannopoulos, Rev. Mod. Phys.* **Vol. 64**, p. 1045 (1992).

14. J. P. Perdew, K. Burke, M. EmZerhof, *Generalized gradient approximation made simple*, *Phys. Rev. Lett.* **vol.77**, no 18, p.3865 (1996).

15. H. J. Monkhorst, and J. D. Pack, *Special points for Brillouin-zone integrations, Physical review B*, **vol. 13**, no 12, p. 5188 (1976).

16. H. D. MEGAW, *Crystal structure of barium titanate*, *Nature,* **vol. 155**, no 3938, p 484-485, (1945).

17. R. I. Eglitis, *Comparative First-Principles Calculations of SrTiO3, BaTiO3, PbTiO3 and CaTiO3 (001),(011) and (111) Surfaces,. Ferroelectrics* , **vol. 483**, no 1, p. 53-67, (2015)

18. B. J. Kennedy, C. J. Howard, B. C. Chakoumakos, *Phase transitions in perovskite at elevated temperatures-a powder neutron diffraction study, J. Phys: Condens. Matter*, **vol. 11**, no 6, p. 1479, (1999).

19. C. B. Samantary, H. Sim, H. Hwang, *Electronic structure and optical properties of barium strontium titanate ($Ba_xSr_{1-x}TiO_3$) using first-principles method* , *Physica B Condensed Matter* **vol. 351**, no 1-2, p. 158-162. (2004).

20. M. M. Rashad, A. O. Turky, A. T.Kandil, *Optical and electrical properties of Ba_{1-x} Sr_x TiO_3 nanopowders at different Sr^{2+} ion content*, *Journal of Materials Science: Materials in Electronics*, **vol. 24**, no 9, p. 3284-3291, (2013).

21. S. Saha, T. P. Sinha, A. Mookerjee, *Electronic structure, chemical bonding, and optical properties of paraelectric $BaTiO_3$*, *Physical Review B*, **vol. 62**, no 13, p. 8828. (2000).

22. S. Saha, T. P. Sinha, A.Mookerjee, *Structural and optical properties of paraelectric $SrTiO_3$, Journal of Physics: Condensed Matter*, **vol. 12**, no 14, p. 3325, (2000).

23. R. Ahuja, O. Eriksson, B. Johansson, *Electronic and optical properties of $BaTiO_3$ and $SrTiO_3$*, *Journal of Applied Physics*, **vol. 90**, no 4, p. 1854-1859, (2001).

24. S. Piskunov, E. Heifets, R. I. Eglitis, G. Borstel, *Bulk properties and electronic structure of $SrTiO_3$, $BaTiO_3$, $PbTiO_3$ perovskites: an ab initio HF/DFT study. Computational Materials Science,* **vol. 29**, no 2, p. 165-178. (2004).

25. H. Lee, T. Mizoguchi, T. Yamamoto, Y. Ikuhara, *First principles study on intrinsic vacancies in cubic and orthorhombic $CaTiO_3$*, *Materials transactions*, **vol. 50**, no 5, p. 977-983, (2009).

26. S. H. Wemple, *Polarization Fluctuations and the Optical-Absorption Edge in $BaTiO_3$*, *Physical Review B* , **vol. 2**, no 7, p. 2679, (1970).

27. K. Ueda, H. Yanagi, R. Noshiro, H. Hosono, H. Kawazoe, *Vacuum ultraviolet reflectance and electron energy loss spectra of $CaTiO_3$*, *Journal of Physics: Condensed Matter*, **vol. 10,** no 16, p. 3669. (1998).

28. K. Van Benthem, C. Elsasser, R. H. French, *Bulk electronic structure of $SrTiO_3$: experiment and theory. Journal of applied physics*, **vol. 90**, no 12, p. 6156-6164, (2001).

29. M. K. Y. Chan, G. Ceder, *Efficient band gap prediction for solids*, *Phys. Rev. Lett.* **vol. 105**, no 19, p. 196403. (2010).

30. R. W. Godby, M. Schlüter, L. J. Sham, *Quasiparticle energies in GaAs and AlAs*, *Phys. Rev*. B, **vol. 35**, no 8, p. 4170. (1987).

31. C. S. Wang, W.E. Pickett, *Density-functional theory of excitation spectra of semiconductors: application to Si, Phys. Rev. Lett.* **vol. 51**, no 7, p. 597 (1983).

32. H. A. Kramers, *The quantum theory of dispersion, Nature,* **vol. 114**, no 2861, p. 310. (1924)

33. R. D. L. KRONIG, *On the theory of dispersion of x-rays, Josa,* **vol. 12**, no 6, p. 547-557. (1926)

34. M. Cardona, *Optical Properties and Band Structure of $SrTiO_3$ and $BaTiO_3$*, *Physical Review*, **vol. 140**, no 2A, p. A651. (1965)

35. D. Bäuerle, W. Braun, V. Saile, G. Sprüssel, E. E. Koch, *Vacuum ultraviolet reflectivity and band structure of $SrTiO_3$ and $BaTiO_3$*, *Zeitschrift für Physik B Condensed Matter*, **vol. 29**, no 3, p. 179-184, (1978).

36. M. Dresselhaus, G. Dresselhaus, S. B. Cronin, A.G. Souza Filho, *Drude Theory–Free Carrier Contribution to the Optical Properties. In Solid State Properties, Springer-Verlag Berlin Heidelberg,* pp. 329-344. (2018)